Nuclear Instruments and Methods in Physics Research A 620 (2010) 401–409

Contents lists available at ScienceDirect

Nuclear Instruments and Methods in Physics Research A

journal homepage: www.elsevier.com/locate/nima

A system for differential neutron scattering experiments in the energy range from 0.5 to 20 MeV

F.J. Saglime [a,*], Y. Danon [a], R.C. Block [a], M.J. Rapp [a], R.M. Bahran [a], G. Leinweber [b], D.P. Barry [b], N.J. Drindak [b,1]

[a] Rensselaer Polytechnic Institute, Department of Mechanical, Aerospace, and Nuclear Engineering, Troy, NY 12180-3590, USA
[b] Knolls Atomic Power Laboratory, P.O. Box 1072, Schenectady, NY 12301-1072, USA

ARTICLE INFO

Article history:
Received 21 September 2009
Received in revised form
4 March 2010
Accepted 15 April 2010
Available online 27 May 2010

Keywords:
Scattering
Neutron
Benchmark
Detection

ABSTRACT

In order to aid in the improvement of the high energy neutron differential scattering cross-section data, scattering experiments were performed using a collimated source of pulsed neutrons with energies up to 20 MeV from the Rensselaer Polytechnic Institute Linear Accelerator. An array of proton recoil detectors surrounding a sample placed at 30.1 m from the source measures the scattered flux using time-of-flight (TOF) methods. A state of the art digital data acquisition system is used to collect the data from the detector array and stream the digitized data to disk. Software was developed to perform pulse shape analysis, multi-channel analyzer functions, and to generate TOF spectra and angular dependent scattered neutron distributions. Scattering measurements were performed on carbon and molybdenum and compared to the Monte Carlo simulation using various nuclear data libraries.

1. Introduction

Neutron differential scattering cross-section data are available from several nuclear data libraries (ENDF [1], JEFF [2], JENDL [3]). These evaluations are based on a combination of theory and a limited number of experiments. Applications involving particle accelerators and advanced nuclear reactors are increasingly driving the need for improved high energy (>1 MeV) nuclear data [4]. In this energy range, the scattering angular distribution shapes are no longer isotropic and can become quite complicated.

The angular distributions of fast neutrons scattering from elements and isotopes have been directly measured by a series of experiments done at Argonne National Laboratory (ANL) [5,6]. These experiments were done with a thin sample using a Van de Graaff accelerator as a pulsed mono-energetic neutron source. Therefore, it was necessary to change the experimental geometry for each energy point. Although, in principle, this may be an ideal way to obtain scattering data, the series of experiments was both difficult and time consuming to perform and has a gap in achievable energies between 8 and 13 MeV [7,8]. Other scattering experiments, which are easier to perform, have been done with detectors placed around a sample using mono-energetic pulsed deuterium–tritium (D–T) sources. The Lawrence Livermore National Laboratory (LLNL) pulsed sphere experiment [9], fusion neutronics source (FNS) [10,11], and Oktavian [12] use a mono-energetic 14.2 MeV D–T pulsed neutron source. In these experiments, the initial pulse of high energy neutrons interact in the sample material, slow down, and eventually leak out, where they are sensed by the detectors far enough away from the sample to allow time-of-flight (TOF) measurements of the leakage flux. In such a configuration, the inverse problem of finding differential scattering cross-sections becomes unmanageable due to the large number of interactions. The primary advantage of the integral experiments done with D–T sources is the sensitivity of these measurements to small errors in cross-section. These experiments have the potential of revealing small discrepancies in nuclear data. But, since the high energy neutrons must undergo numerous collisions to reach lower energies, little direct information about the angular distribution of the cross-sections can be extracted.

Another related experiment is the FIGARO [7,13] at Los Alamos National Laboratory (LANL). This experiment uses a pulsed spallation neutron source, and therefore has a continuous energy distribution of neutron energies produced. Energy is resolved using the TOF method. Both gamma and neutron detectors are placed around the scattering sample. Using the resulting gamma and neutron emission spectra from inelastic scattering, information on the level density of states of the nucleus in the scatterer is obtained. This experiment is more similar to the present work in terms of the experimental setup than the previously mentioned experiments, but is primarily being used to obtain level density information of excited states of the target nuclei.

A new experimental capability, the high energy scattering system (HESS) at the Rensselaer Polytechnic Institute (RPI) linear

* Corresponding author. Tel.: +1 518 892 9967.
E-mail address: franksaglime@mac.com (F.J. Saglime).
[1] Retired.

0168-9002/$ - see front matter © 2010 Elsevier B.V. All rights reserved.
doi:10.1016/j.nima.2010.04.051

accelerator (LINAC) facility, is able to provide benchmark quality data to evaluate nuclear data libraries. The results from the HESS experiment can easily identify neutron energy regions of materials that need to be addressed and guide the performance of other experiments. The main difference of the present experiment from the D–T based experiments is in the use of a white source. By using the TOF method, it is possible to measure scattering spectra for which the principle component comes from single scattering events over a wide range of energies. The amount of multiple scattering can be controlled by the thickness of the scattering sample. The advantage of this experiment is the ability to do quasi-differential benchmark experiments, which give results that are still sensitive to the differential scattering cross-section over a continuous distribution of energies (0.5–20 MeV).

2. Experimental setup

2.1. Arrangement

The experimental setup was placed at a distance of 30.07 m ($\pm$0.02 m) from the neutron source. The LINAC was used to produce neutrons [14]. High energy (50–60 MeV) electrons collided with a water cooled tantalum assembly (the target) in a heavily shielded room. These electrons rapidly lose energy in the tantalum by Coulombic interactions generating Bremsstrahlung radiation, which in turn interacts through (γ, n) reactions to produce the desired neutrons. The energy distribution of the source neutrons could be approximated by an evaporation spectrum with a 0.5 MeV temperature but needed to be more accurately characterized for the purposes of this experiment (see Section 3.2).

This pulse source is capable of generating between 10^{11} and 10^{12} n/sec in 5 ns bursts with 6 μA of average current at a repetition rate of 400 Hz. Fig. 1 shows the present experimental arrangement. With a hole in the target room wall, a collimation system was used to form a 7.62 cm (3 in.) diameter beam of neutrons at the sample location, and a 2.54 cm (1 in.) thick piece of depleted uranium was used to attenuate the intense gamma flash.

With the sample placed in the beam path at 30.07 m ($\pm$0.02 m), an array of eight proton recoil detectors were arranged around the sample at measured angles of 26, 52, 72, 90, 107, 119, 140, and 154° ($\pm$2°), as shown in Fig. 2 (angles less than 26° and greater than 154° put part or all of the detector in the beam). Each detector was placed 50 cm ($\pm$2 cm) from the center of mass of the sample with the exact distance measured to within 0.1 cm. The detectors are arranged in 3D to maximize the distance between detectors, thus minimizing the crosstalk. The detectors were securely mounted on a 152 × 152 cm (5 × 5 ft) optical table using 3.81 cm (1.5 in.) dia. aluminum tubing, a stanchion mounting block to attach to the table, a cross-clamp, and special detector mounting hardware with a U-joint to allow

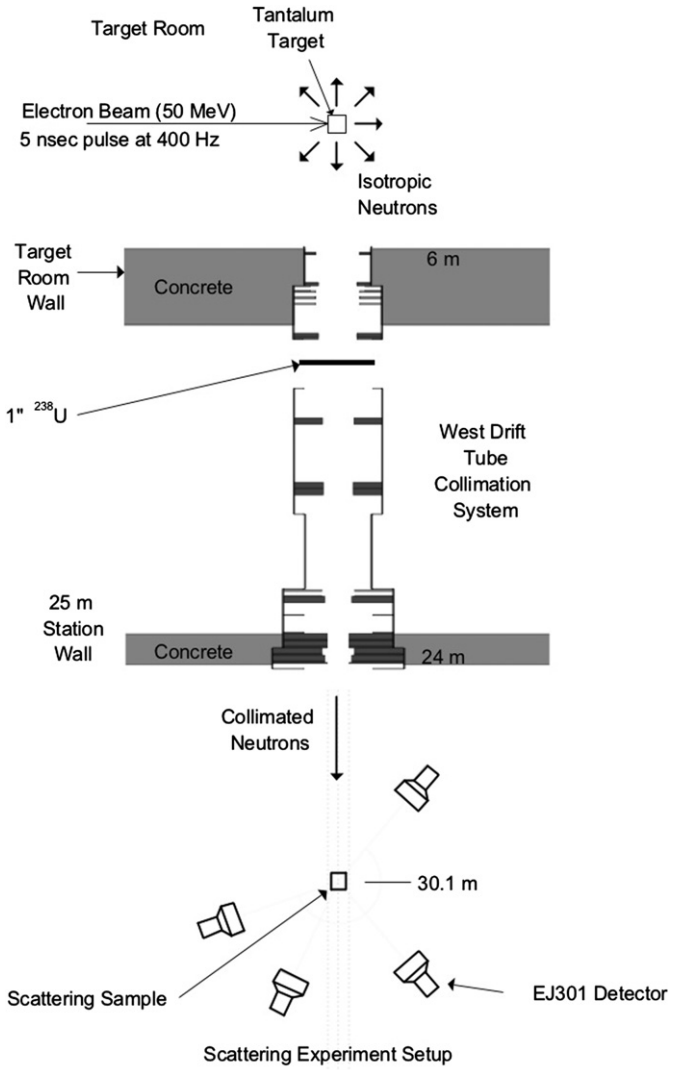

Fig. 1. Overview of the scattering experimental setup in the Rensselaer Polytechnic Institute (RPI) linear accelerator (LINAC) facility. Note: not to scale, and only four of the eight detectors are shown for simplicity.

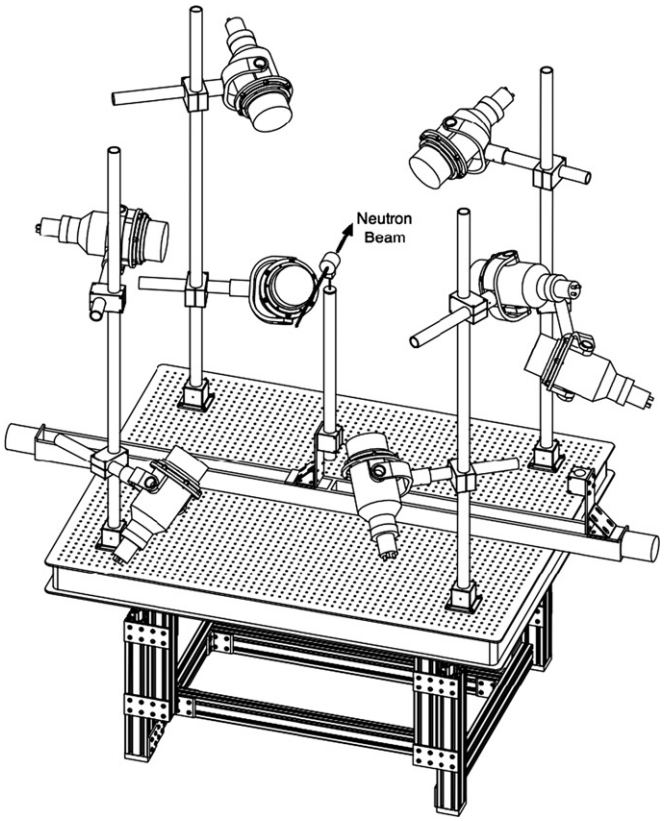

Fig. 2. Detailed view of the scattering experiment detector array. Detectors are secured in the proper positions through 3.81 cm (1.5 in.) dia. aluminum rod attached to 152 × 152 cm (5 ft × 5 ft) optical table.

Table 1
Sample dimensions and number density.

Sample	Thickness (cm)	Diameter (cm)	Mass (g)	Number density (atoms/b)
Carbon	7	7.493 ± 0.003	521.87 ± 0.01	0.5924 ± 0.0002
Molybdenum	8	7.616 ± 0.001	3713.4 ± 0.1	0.51184 ± 0.00013

for an additional degree of freedom. Extruded aluminum legs that allow for height adjustment support the optical table. A 7.49 cm dia. $\times$ 7 cm solid piece of graphite (see Table 1) was used to scatter neutrons [15]. The thickness was selected to maximize the scattering yield at 26°. A remotely controlled motorized sample changer was used to move two mounted samples in and out of the beam (only one sample is shown in Fig. 2).

2.2. Measurement

Raw data from the detector array were collected using the Acqiris AP240 digitizers sampling at 1 GHz and streamed to disk for later analysis. A 5 in. dia. $\times$ 3 in. long EJ301 [16] detector (combined scintillator photomultiplier from ELJEN Technologies Model no. 510-50 $\times$ 30-5/301) was used for neutron detection [17,18]. High voltage was supplied to the detectors by a CAEN 1733 N. Actual anode MCA spectra were taken using a ^{22}Na source. The detector high voltage was used to control the size of the pulses from the anode such that the Compton edge of 0.511 MeV gammas corresponded to 580 mV pulses. All channels of the digitizers and detectors were configured identically (gain matched by adjusting the detector high voltage).

In this experimental setup, the software takes the place of traditional hardware used in radiation detection systems such as amplifiers, filters, integrators, discriminators, etc. Algorithms within data analysis programs perform this functionality. Two sets of programs were created: data acquisition and data analysis. All programs were coded in C++. The data acquisition software uses the National Instruments Measurement Studio tools, and the data analysis software uses the ROOT [19] for analysis and plotting functionality.

The background was measured with only the sample holder in the beam while the LINAC was operating the 'sample out' position [24]. The effect of LINAC beam intensity fluctuations was accounted using monitor detectors (two fission chambers located at the target room wall, 8.7 m from the tantalum target on a separate beam line, and a Li-6 glass ring detector at 9 m). Normalization was accomplished by dividing the TOF spectra by the monitor counts. To minimize the effect of LINAC beam fluctuations on the data, scattering measurements and background measurements were made by repeatedly alternating between sample in and sample out. The effect of the background was removed by subtraction of the background spectra from the acquired scattering spectra.

2.3. Data processing

Use of intelligent data transfer techniques between the digitizer and the computer minimized the transfer and storage requirements by passing only the data in the vicinity of the detector pulse. The system was designed to run under Windows XP and is capable of digitizing 120 ns of data per pulse at a 1.0 ns sampling interval; it is capable of handling 128,000 events/s in conjunction with other tasks, but is capable of nearly twice this if the data acquisition program is the only task running. The dead time of the system is characterized by the sampling duration of a detected pulse (120 ns).

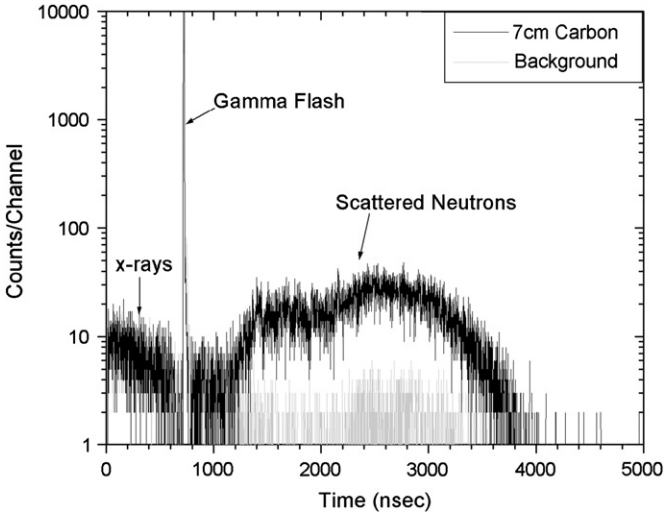

Fig. 3. Raw experimental data (before pulse shape discrimination is applied) with 1 nsec channels for a single run at 26° showing a comparison of the carbon scatterer counts to background counts (17:1 in the scattered neutron region).

After the data were collected, each pulse was analyzed to classify it as a gamma or a neutron event. A computationally efficient least squares algorithm was developed to fit the fast and slow component shapes of the scintillator to the detected pulse. Using the ratio of the magnitude of the slow and fast components, it was possible to determine if the incident particle was a gamma or a neutron [20]. This was necessary since both gammas (from inelastic scattering) and neutrons are present in the scattered flux. More traditional techniques measured only the fall time of the pulse to distinguish the type of the particle. There is a one-to-one correspondence between the slow/fast ratio and the fall time given by other existing laboratory instruments. For historical reasons, and for compatibility with these other instruments, the data are presented in terms of fall time. The ability to distinguish between gammas and neutrons using a Pu–Be source as a function of fall time with various software discriminator levels is shown in Fig. 3. Better separation is achieved with higher discriminator levels. A two-dimensional discrimination technique using both pulse height and fall time was used to identify neutrons with a low discriminator level. Fig. 4 shows a detector in the beam analyzed this way, and Fig. 5 shows a pure gamma source (Na-22) where only 2% of the gamma pulses fall within the neutron window. By excluding the region where gamma pulses overlap with neutrons (see Fig. 6), an overall lower pulse height discriminator level can be used, which minimizes the false positive error rate at the same time. Furthermore, it is possible to have the discriminator level be a function of the TOF since the computer does the analysis after the data have been collected.

For a given angle, the scattered neutron TOF spectrum was created using the time stamp of the neutron pulses. A histogram with 5 ns bins was created using all the neutron data from the

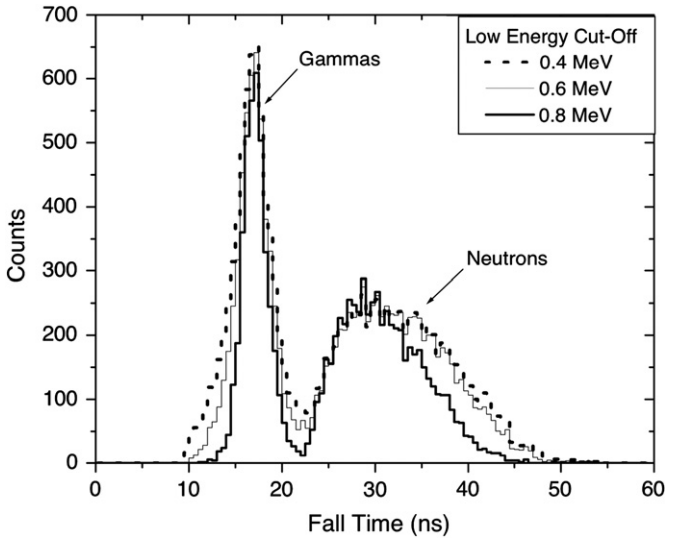

Fig. 4. Pulse shape discrimination (PSD) fall-time histograms demonstrating the ability of the system to distinguish between gammas and neutrons using a PuBe source with software generated low energy cutoff discrimination levels of 0.4, 0.6, and 0.8 MeV. Note that higher discriminator levels give better separation between gamma and neutrons.

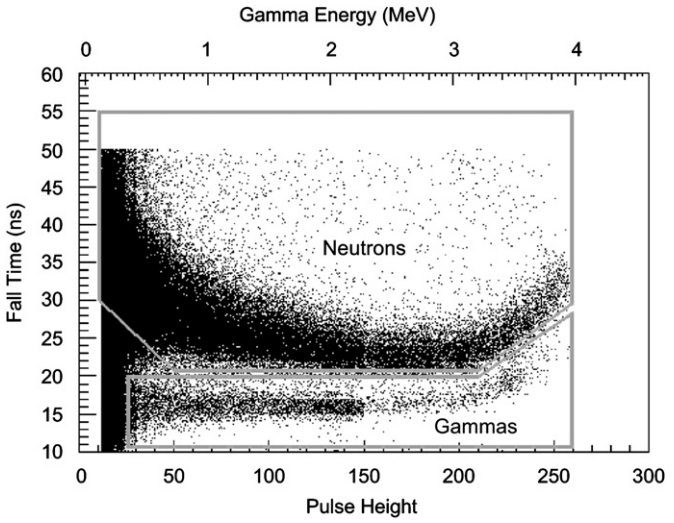

Fig. 5. Fall time versus pulse height shows the separation between gamma rays and neutrons with the energy scale (top axis) shown for gammas. The detector was placed in the beam of the RPI LINAC using the bare tantalum target where both neutrons and gammas are generated. A 2.2 MeV gamma from hydrogen capture can be clearly seen by the change in the point density in the gamma events region. The software tools use a polygon based discrimination technique. Points falling within the upper grey polygon were identified as neutrons, and the points falling within the lower polygon were identified as gammas.

experiment. The gammas from inelastic scattering and other sources were also present in the raw data making up 6% of the total, but the current work separated out this component; only 0.1% of the neutron data are from gamma contamination. The other source of gammas comes from the target itself when the electrons interact in the target. This gamma flash can not only interfere with detector recovery but also serves as a convenient marker in the data to aid in finding t_0 (when the electrons strike the target) to get the correct timing for the experiment. To eliminate gamma flash associated recovery issues, 2.54 cm (1 in.) of depleted uranium was placed in the beam at the opening in the collimation system as shown in Fig. 1.

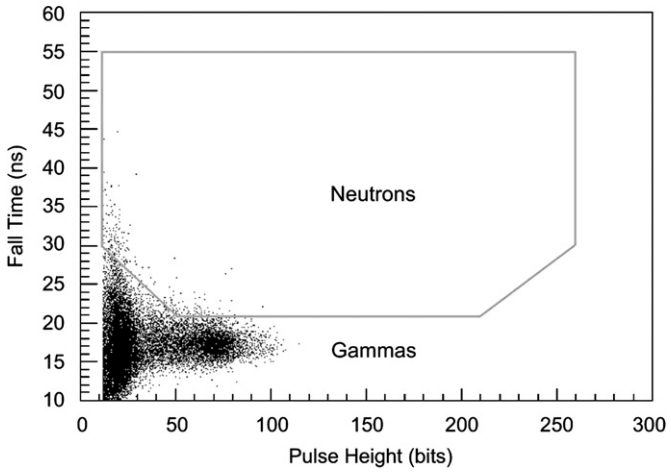

Fig. 6. Fall time versus pulse height for Na-22. A pure gamma source shows why the neutron polygon in Fig. 4 is set with a notch taken out for low pulse heights. The effect of digitization and noise on small pulses causes more error on the fall-time calculation and spreading on the scatter plot.

3. Analysis

If one knows the differential scattering cross-sections for the scatterer, the incident flux, and the detector efficiency, it is possible to calculate/simulate the detector response to the scattered neutrons. Therefore, if a material with a well known cross-section (such as carbon) is used as a scatterer and the experimental data match the calculation/simulation, the experimental method would be considered validated. Then, other materials can be studied using the same experimental technique with implications for that material's differential scattering cross-section obtained from the comparison of simulation to experiment.

3.1. Detector efficiency

The detector efficiency was found using SCINFUL, a Monte Carlo code for determining the efficiency of proton recoil detectors [21,22]. The calculated pulse height spectra for different energies are shown in Fig. 7 where the effect of a small dynamic range of the data acquisition system is noted by a vertical line. The calculated detector efficiency is shown in Fig. 8, and was checked experimentally below 2 MeV by an in-beam LINAC detector measurement (allowing for TOF energy measurements) compared to a ^{6}Li glass detector measurement of the same flux using an MCNP calculated efficiency. Pulses that over ranged the analog to digital converter (ADC), i.e. corresponding to pulses above the ADC saturation in Fig. 7, were rejected since pulse shape analysis cannot be done on these pulses with the current algorithms. This led to a lower efficiency, which can also be seen in Fig. 8. The errors in the efficiency were estimated from the comparisons with experimental data from the SCINFUL documentation [19].

3.2. Incident flux

In order to predict the scattered neutron flux, one must know the incident flux; for this reason, much care was taken in its measurement. The energy spectrum of the neutrons produced by the LINAC spans an energy range greater than a single detector can accurately measure. Two detectors with an overlapping energy range were used. The flux measurement is obtained at each energy point using an EJ301 (proton recoil) flux measurement and a ^{6}Li glass [23] (n,α) measurement combined

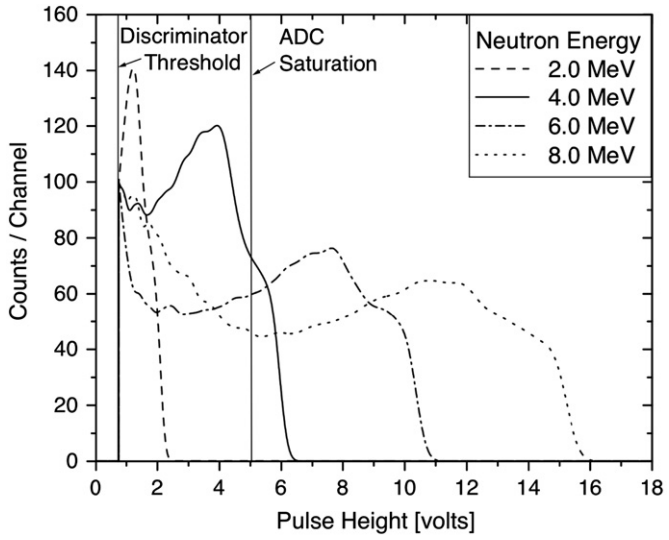

Fig. 7. Calculated pulse height spectrum from SCINFUL [18] for multiple neutron energies relative to discriminator threshold and ADC saturation. Pulse heights are calculated in volts at the anode output of the photomultiplier on the EJ301 detector.

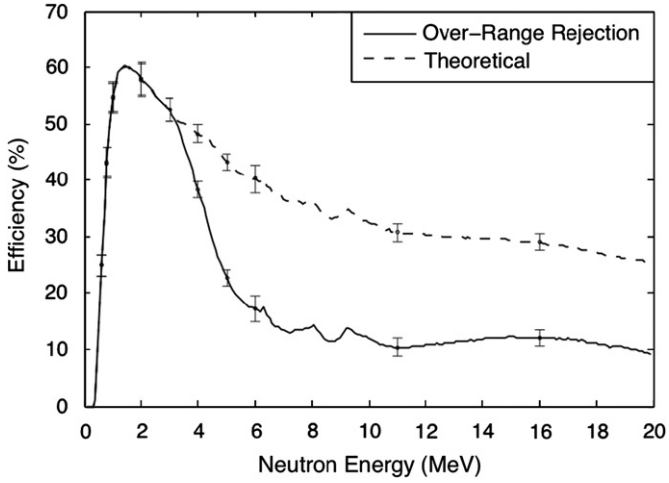

Fig. 8. Calculated EJ301 detector efficiency with the effect of ADC saturation. Since the pulse shape discrimination cannot be applied to over-ranged pulse data, the efficiency of the data analyzed using it will be reduced. The theoretical efficiency from SCINFUL [18] is the efficiency with only the discriminator level accounted for; this efficiency will include over-ranged pulses. The over-range rejection efficiency is the efficiency that is obtained when these pulses are rejected.

in such a way so as to minimize the error for each point [24]. Above 2 MeV, the error in this measurement is dominated by the efficiency error (and not the counting statistics) associated with the EJ301 detector. Below 0.5 MeV, the error is dominated by the error in the efficiency of the ^{6}Li glass detector (conservatively taken as 5%). In the region of overlap, between 0.5 and 2.0 MeV, the measurements were normalized to each other.

In order to reduce the gamma flash, the neutron flux was measured through a one inch thick piece of depleted uranium. By a simple calculation given by Eq. (1), it is possible to determine the energy spectrum of the bare target.

$$\Phi'(E) = \Phi(E)e^{-\Sigma_{U238}(E)L_{U238}} \quad (1)$$

where E is the energy, $\Phi'(E)$ the energy dependent flux at the scattering sample, $\Phi(E)$ the energy dependent flux at the target, $\Sigma_{U238}(E)$ the energy dependent macroscopic total cross-section of depleted uranium, and L_{U238} the thickness of the uranium.

Table 2
Target energy spectrum evaporation temperatures.

Weight w_i	Evaporation temp. E_{T_i} (MeV)
0.0960	0.05
0.3520	0.25
0.7039	0.52
0.0896	1.60
0.0576	3.00

The bare target's energy spectrum is a continuous spectrum of evaporation spectra over a narrow energy range (usually a single evaporation spectrum is used with a temperature corresponding to the dipole resonance energy) [25–27], but can be closely approximated by a sum of five evaporation spectra given by Eq. (2).

$$\Phi(E) = \sum_{i=1}^{5} w_i \left(\frac{E}{E_{T_i}^2} \exp\left(\frac{-E}{E_{T_i}} \right) \right) \quad (2)$$

The values for the weights and evaporation temperatures given in Table 2 were selected to match the experimental in-beam data. This flux, transmitted through the piece of depleted uranium, the air in the target room, and the air in the 25 m station, is shown in TOF at the scatterer in Fig. 9.

3.3. Monte Carlo simulation

The geometry, neutron flux energy distribution, and detector efficiency information were input to a Monte Carlo code (MCNP5 [28]) to simulate the entire scattering experiment. Several effects were simulated in the MCNP model including the transmission and scattering in air, detector efficiency, and size, but the detectors themselves were not modeled, so scattering from the detectors was not included. An array of point detectors ('f5' tally) with a uniform point density were used to simulate the detector volume (at the proper location), and 'de' and 'df' cards were used to enter the SCINFUL calculated efficiency and give counts per source neutron in the output file. This simulation predicts the TOF spectra for the scatterer used, and can be directly compared with measurements done at specific detector angles. An MCNP simulation that tallied scatters off of a liquid scintillator cell at 90° and an aluminum table cell showed less than 0.5% of the experiment simulation tally; so secondary contributions from the experimental setup were neglected.

4. Results

In the desired energy range, carbon has a total cross-section, which has been extensively measured and for which all evaluations agree. Recent high precision measurements of the total cross-section provide additional verification of the ENDF/B[1] total cross-section for this material [29]. Validation of the HESS was accomplished by comparing the simulated results to the experimental results for carbon measurements.

The total cross-section and the differential scattering cross-section of carbon have structures in the 2–10 MeV range resulting in complicated TOF spectra. Therefore, the results from the transport model were sensitive to the characterization of the differential scattering distribution. This unique pattern in the detector response provided a way to test the timing and

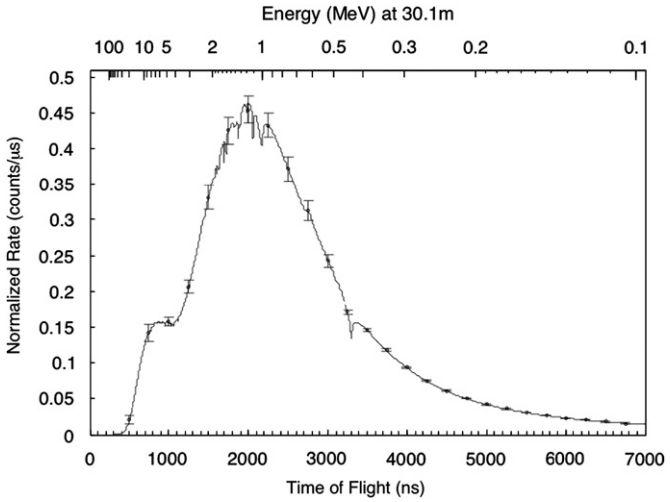

Fig. 9. Combined In-beam neutron flux measurement from EJ301 and Li-6 glass detectors at 30.1 m with 1 in. of depleted uranium in the beam line. (curve normalized to area = 1).

resolution of the data collection system since key resonances could easily be identified. Figs. 10 and 11 show the experimental and simulation results together; they are in quite good agreement. The structure in the detector response below 2 MeV is a result of neutron interaction with air, which the neutrons pass through before striking the carbon, and must be accounted for in the simulation. Below 1 MeV, the efficiency of the detector falls off rapidly and has a cutoff at about 0.5 MeV. As a result, the detector response goes to zero even though neutrons as low as 0.1 MeV are actually present. The structure above 2 MeV comes from the carbon. This structure is best seen at forward and backward angles. The structure that can be seen in these data is in the form of peaks, but there is structure, in the form of sharp dips, which is masked by the amount of multiple scattering that takes place in this sample. Such dips in the spectra would be visible at certain angles if thin scattering samples were used for this material.

The MCNP simulation contains all the same features, and correlates with the detector data. The only exception is at 154° (see Fig. 11), which shows some discrepancy at the low energy edge, which is most likely caused by a small error in detector

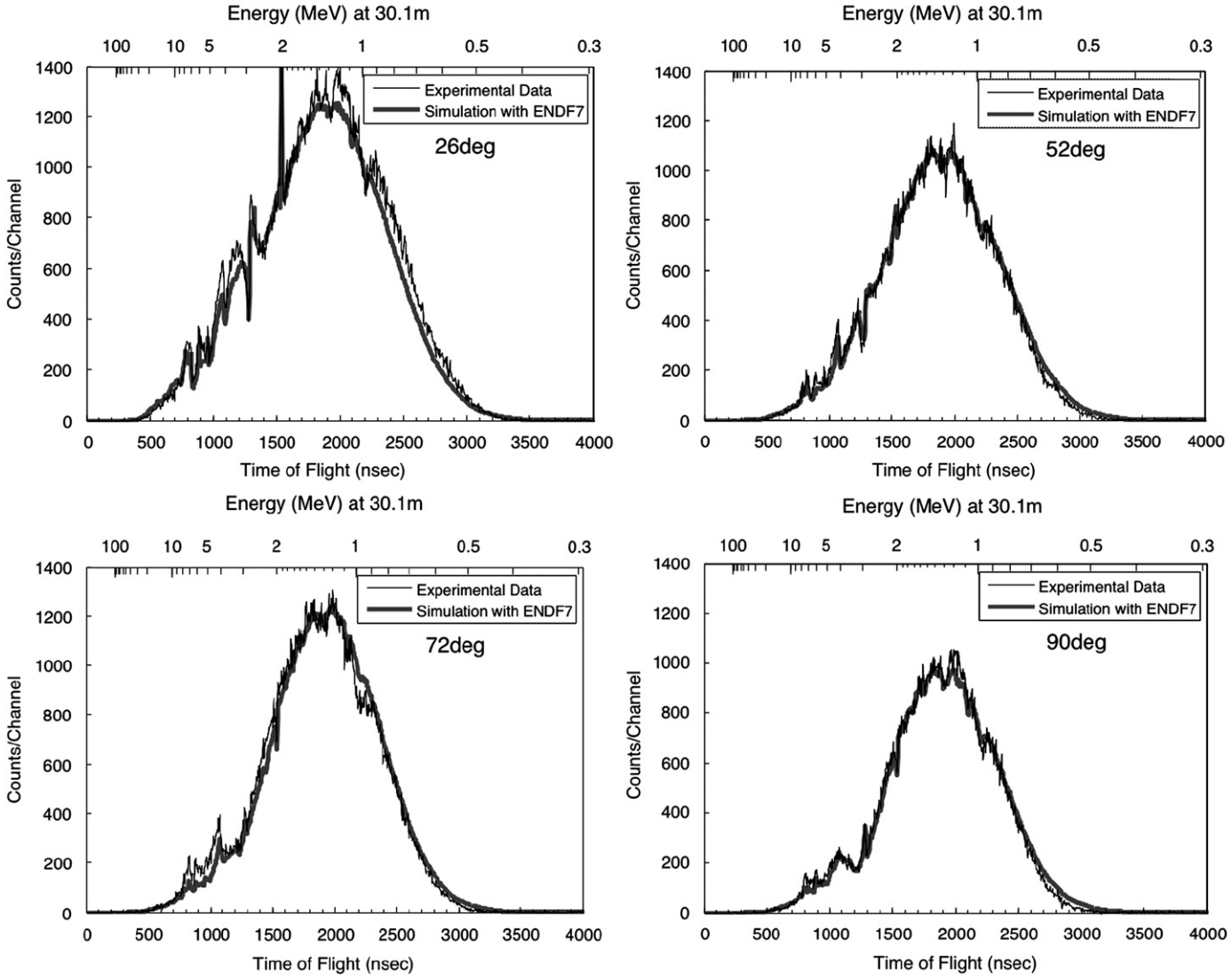

Fig. 10. Carbon (7.62 cm (3 in.) dia. × 7 cm (2.76 in.)) neutron scattering measurements at 26°, 52°, 72°, and 90°.

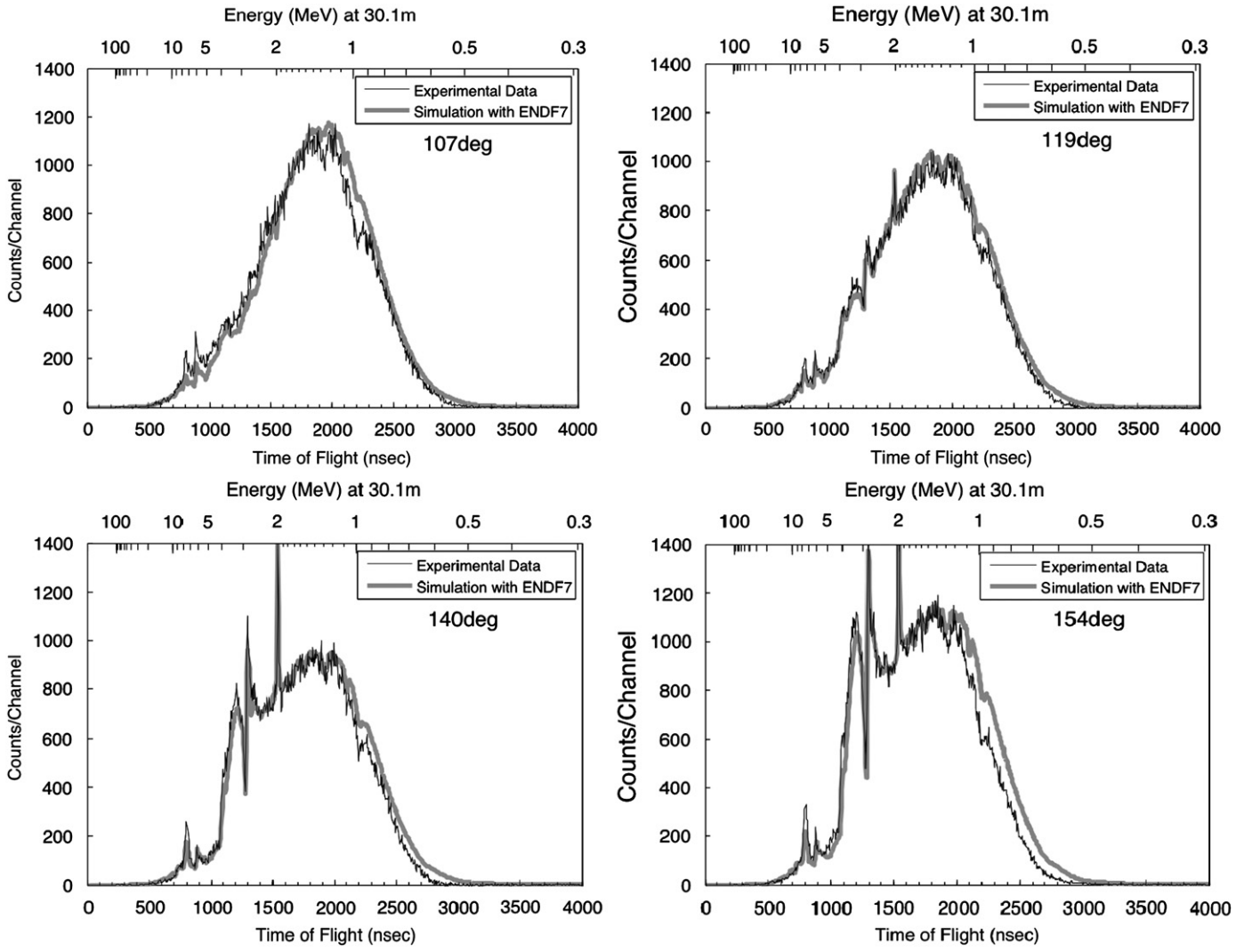

Fig. 11. Carbon (7.62 cm (3 in.) dia. × 7 cm (2.76 in.)) neutron scattering measurements at 107°, 119°, 140°, and 154°.

discriminator alignment. Comparison of the MCNP simulation with the experimental results will highlight energy and angular regions where the nuclear data used for the simulation can be improved.

Fig. 12 shows the results of a scattering experiment done with molybdenum (see Table 1) compared to the MCNP simulation using ENDF/B (other libraries give nearly identical results to ENDF/B). Although the results are in good general agreement, the differences for molybdenum ENDF/B 6.8 are greater than that of ENDF/B 7.0 suggesting that the improvements made in this evaluation more closely reflect the reality. This illustrates the utility of the system; however, the implication for differential scattering cross-section of molybdenum is beyond the scope of the current discussion and will be the subject of a future paper.

5. Discussion and conclusions

The ability to digitize the entire experiment at the output of the detectors offers the ability to examine the data in a number of different ways after the conclusion of the experiment. The data may be re-analyzed with new and improved algorithms to refine older results. Or it may be possible to look for new information in older experiments without actually re-running the experiment, thus providing a significant cost savings.

The method proposed here uses a combination of the Monte Carlo calculation and experiment to assess differences in the scattering cross-section evaluations. The Monte Carlo code is required to accurately model the experimental setup including the neutron source, detector efficiency, and the time dependent neutron transport in the sample and the rest of the system. As was shown, a combination of MCNP and SCINFUL provided results that were in excellent agreement with carbon data and validated the system and methods. This benchmarking method and the HESS can be used to discriminate between nuclear data evaluations for materials of interest at energies between 0.5 and 20 MeV where there are differences in the angular distributions for the differential scattering cross-sections. In addition to elemental samples, heterogeneous and composite materials can easily be accommodated as well. This system is being considered to study fission neutron angular distribution and yield by using a fissile material target and a fission event tag.

Ongoing work at the LINAC to improve the source strength can allow thinner samples to be used. This would reduce the amount of multiple scattering, opening up the possibility for direct differential scattering measurements over a wide range of energies in one experiment.

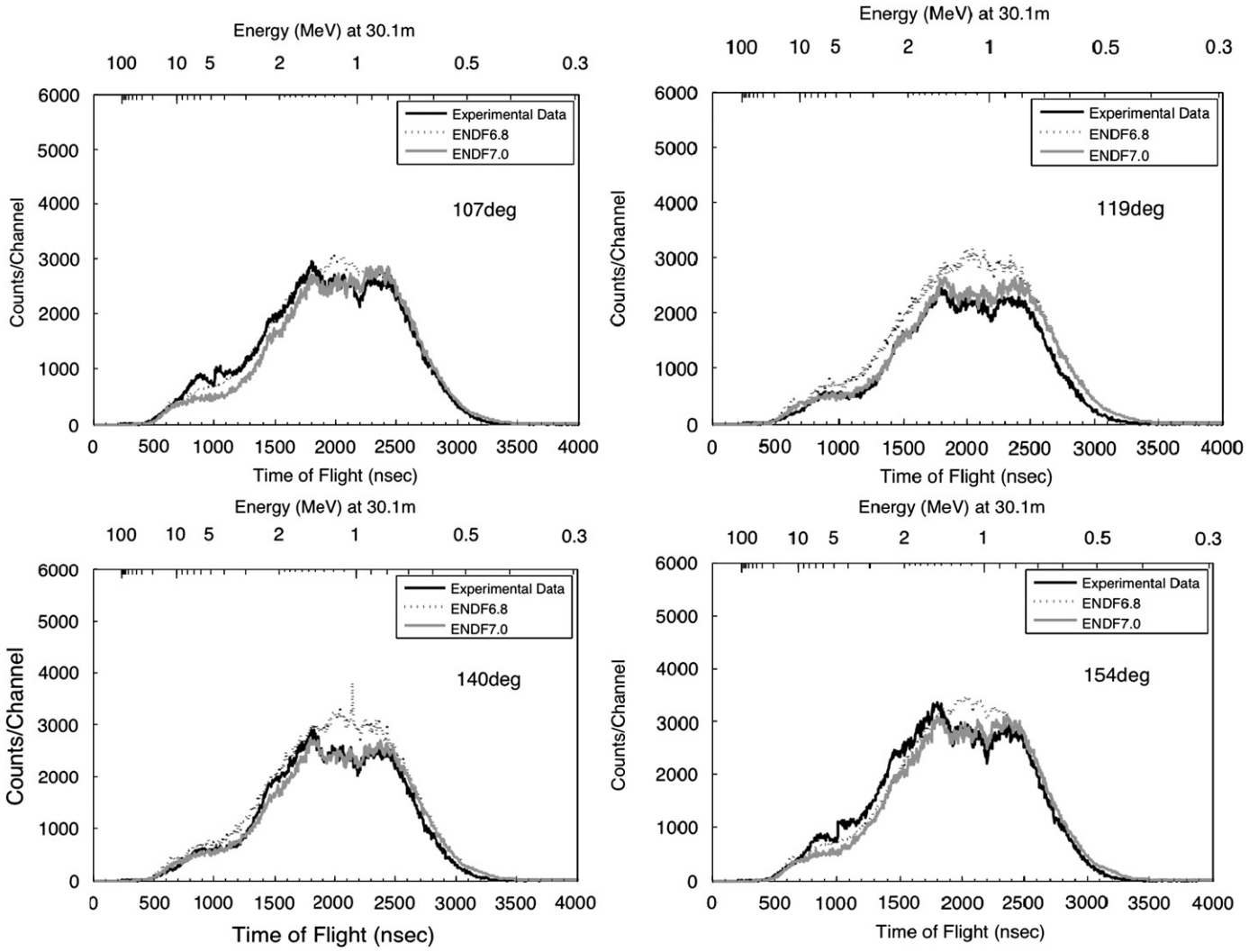

Fig. 12. Molybdenum (7.62 cm (3 in.) dia. × 8 cm (3.15 in.)) neutron scattering measurements at 107°, 119°, 140°, and 154°. The difference between the dotted black line and the solid grey line shows the difference between the MCNP simulated benchmark using the ENDF/B 6.8 and 7.0 cross-sections for molybdenum. The solid black line is the result from experiment.

Acknowledgment

The authors would like to thank the RPI LINAC operators and staff: Peter Brand, Mathew Grey, Martin Strock and Azeddine Kerdoun.

References

[1] M.B. Chadwick, P. Oblozinski, M. Herman, et al., Nucl. Data Sheets 107 (2006) 2931.
[2] A. Koning, R. Forrest M. Kellett et al., Nucl. Energy Agency, 92-64-02314-32006.
[3] K. Shibata, Ed., Descriptive Data of JENDL-3.3 (Part I and II), JAERI-Data/Code 2002–026, 2003.
[4] D. Schmidt, Nucl. Sci. Eng. 160 (2008) 349.
[5] A.B. Smith, R. Holt, J. Whalen, Argonne National Laboratory Report, ANL/NDM-43, 1978.
[6] A. Smith, P. Guenther, Argonne National Laboratory Report, ANL/NDM-76, 1982.
[7] R.C. Haight, J.M. O'donnell, L. Zanini, M. Devlin, D. Rochman, FIGARO: measuring neutron emission spectra with a white neutron source, Los Alamos National Laboratory Report, LA-UR-02-5486, 2002.
[8] D. Rochman, et al., Nucl. Instr. and Meth. A 523 (2004) 102.
[9] C. Wong, J.D. Anderson, P. Brown, L.F. Hansen, J.L. Kammerdiener, UCRL-51144 Rev. 1 (1972).
[10] Y. Oyama, S. Yamaguchi, H. Maekawa, J. Nucl. Sci. Technol. 25 (1988) 419.
[11] F. Maekawa, C. Konno, Y. Kasugai, Y. Oyama, Y. Ikeda, Data collection of fusion neutronics benchmark experiment conducted at FNS/JAEA, JAERI-Data/Code 98-021, 1998.
[12] C. Ichihara, A. Hayashi, I. Kimura, J. Yamamoto, A. Takahashi, J. Nucl. Sci. Technol. 37 (4) (2000) 358.
[13] L. Zanini, et al., CAARI, in: AIP Proceedings of the Sixteenth International Conference on the Application of Accelerators in Research and Industry, vol. 576, Denton, TX, USA, 346 pp.
[14] M.E. Overberg, B.E. Moretti, R.E. Slovacek, R.C. Block, Nucl. Instr. and Meth. Phys. Res. **A** 438 (1999) **253**.
[15] Y. Danon, et al., Nucl. Sci. Eng. 161 (2009) 321.
[16] Eljen Technology, EJ-301 Liquid Scintillator 〈http://www.eljentechnology.com/datasheets/EJ301%20data%20sheet.pdf〉.
[17] A. Li, et al., IEEE Nucl. Sci. Symp. Conf. Rec. (2007) 1373.
[18] A. Aksoy, et al., Nucl. Instr. and Meth. Phys. Res. (1994) 486.
[19] R. Brun, F. Rademakers, ROOT an object oriented data analysis framework, root.cern.ch/root, 2004.
[20] S. Marrone, et al., Nucl. Instr. and Meth. Phys. Res. A 490 (2002) 299.
[21] Scintillator full response to neutron detection (SCINFUL), PSR-0267, Oak Ridge National Laboratory, 1988.
[22] J.K. Dickens, Oak Ridge National Laboratory Report 6463, 1988.
[23] D.P. Barry, Neodymium neutron transmission and capture measurements and development of a new transmission detector, Ph.D. Thesis, Rensselaer Polytechnic Institute, 2003.
[24] F. Saglime, High energy nuclear differential scattering measurements for beryllium and molybdenum, Ph.D. Thesis, Rensselaer Polytechnic Institute, 2009.
[25] J.R. Wu, C.C. Chang, Phys. Rev. C16 (1977) 1812.

[26] G.A. Price, Phys. Rev. 93 (1954) 1279.
[27] J.M. Blatt, V.F. Weisskopf, in: Theoretical Nuclear PhysicsJohn Wiley & Sons, 1952.
[28] Mcnp, A General Monte Carlo code for neutron and photon transport, version 5, LA-UR-05-8617, 2005.
[29] M. Rapp, et al, High energy neutron time of flight measurements of carbon and beryllium samples at the RPI LINAC, International Conference on Mathematics, Computational Methods & Reactor Physics (M&C), 2009.